

## PHOTOCATALYTIC REACTOR USING TiO<sub>2</sub> DOPED WITH N AND SnO<sub>2</sub> COATED ON GLASS FIBER FOR CONTAMINATED WATER TREATMENT

P. KONGSONG<sup>a,\*</sup>, L. SIKONG<sup>b</sup>, M. MASAE<sup>c</sup>

<sup>a</sup>*Department of Materials Engineering, Faculty of Engineering and Architecture, Rajamangala University of Technology Isan, Nakhon Ratchasima 30000, Thailand*

<sup>b</sup>*Department of Mining and Materials Engineering, Faculty of Engineering, Prince of Songkla University, Hat Yai, Songkhla, 90112, Thailand*

<sup>c</sup>*Department of Industrial Engineering, Faculty of Engineering, Rajamangala University of Technology Srivijaya, Songkla 90000, Thailand*

This study aimed to investigate the efficiency of glass fiber which has been coated by TiO<sub>2</sub> doping with SnO<sub>2</sub> and nitrogen. TiO<sub>2</sub> films were prepared by sol-gel method and coated on E-glass type of glass fibers by using dip-coating. Then the films were calcined at temperature of 600°C for 2 h. The photodegradation efficiency of harmful chemicals which are humic acid (C<sub>0</sub>=10 mg/L), fulvic acid (C<sub>0</sub>=10 mg/L), 2,4-dichlorophenol (C<sub>0</sub>=10 mg/L) and glyphosate (C<sub>0</sub>=1x10<sup>-4</sup> M) contamination in water were investigated using a photocatalytic reactor containing N-doped SnO<sub>2</sub>/TiO<sub>2</sub> composite films coated on glass fibers. It was found that at the flow rate of 250 mL/min the photo-reactor degradation of humic acid, fulvic acid, glyphosate and 2,4-dichlorophenol contamination in water were 91.30, 95.50, 71.80 and 88.70 %, respectively. It is apparent that TiO<sub>2</sub> composite photocatalytic reactor shows advantages in degradation of some hazardous chemical compounds contamination in water.

(Received May 15, 2018; Accepted July 18, 2018)

*Keywords:* Photocatalytic reactor, N-doped SnO<sub>2</sub>/TiO<sub>2</sub>, Sol-gel methods, Glass fibers, Water treatment

### 1. Introduction

In recent years, photocatalytic oxidation processes have shown great potential as a low-cost, environmental friendly treatment technology in the water and wastewater industry. This oxidation technology has been widely demonstrated to have the ability to remove persistent organic compounds and microorganisms in water [1].

Advanced Oxidation Processes (AOPs) seem to be one of the most promising methods for the removal of various organic contaminants. Among others, photocatalysis has been especially extensively investigated. The most commonly used photocatalyst is titanium dioxide. This is due to the merits revealed by the material such as relatively low cost, high photocatalytic activity, and chemical stability [2].

When applied for water treatment, TiO<sub>2</sub> is utilized in two forms, which are in the form of slurry (or suspension) or, in the immobilized form. The advantage of utilizing the slurry form is larger surface area of TiO<sub>2</sub> nanoparticles compared to the immobilized form. However, the difficulty of the use of the slurry form is post separation treatment of TiO<sub>2</sub> nanoparticles. To immobilize TiO<sub>2</sub> on transparent substrates such as glass or silica gel is alternative approach to apply it for water treatment. Annular photoreactor uses immobilized TiO<sub>2</sub> on the glass surface, with the UV lamp at the center of the reactor. In this method, however, although separation problem is solved, contact surface area of TiO<sub>2</sub> with pollutants is limited. On the other hand,

---

\*Corresponding author: physics\_psu@windowslive.com

packed bed reactor that utilizes TiO<sub>2</sub> coated on silica gel has both of the required properties such as relatively high surface area and good separation performance [3].

In order to enhance the photocatalytic activity of TiO<sub>2</sub> for its practical use and commerce, it is important to decrease the recombination of photogenerated charge carriers. Coupling TiO<sub>2</sub> with other semiconductors can provide a beneficial solution for this drawback. For example, Tada et al. and Kadam et al. [4-5] conducted a systematic research on the SnO<sub>2</sub> as a coupled semiconductor and confirmed that the photogenerated electrons in the SnO<sub>2</sub>/TiO<sub>2</sub> system can accumulate on the SnO<sub>2</sub> and photogenerated holes can accumulate on the TiO<sub>2</sub> because of the formation of heterojunction at the SnO<sub>2</sub>/TiO<sub>2</sub> interface, which can result in lower recombination rate of photogenerated charge carriers and higher quantum efficiency and better photocatalytic activity [6].

Nitrogen-doped titanium dioxide is attracting a continuously increasing attention because of its potential for the material for environmental photocatalysis. While some authors claim that the band gap of the solid is reduced due to a rigid valence band shift upon doping others attribute the observed absorption of visible light by N-TiO<sub>2</sub> to the excitation of electrons from localized impurity states in the band-gap. Interestingly, it appears that the N-doping induced modifications of the electronic structure may be slightly different for the anatase and rutile polymorphs of TiO<sub>2</sub>. The mechanism of N-dopant influence on the photoabsorption and photoactivity was a matter of intensive discussions. Various theoretical and experimental approaches assume band gap narrowing by overlapping between N 2p and O 2p orbitals, e.g. formation of intra-band surface states, oxygen vacancies, demonstrate the complexity of the case and deserved several reviews. It is reminded that N doping is extremely sensitive to the preparation technique and its state and configuration is still in the focus of researcher's attention. A number of investigations of substitutional and interstitial N-doped TiO<sub>2</sub> visible light photocatalytic activity confirms the advantage of interstitial position [7-8].

The aim of this work was to assess the photodegradation efficiency of harmful chemicals which are humic acid (HA), fulvic acid (FA), 2,4-dichlorophenol (2,4-DCP) and glyphosate contaminants in drinking water using a photocatalytic reactor containing N-doped SnO<sub>2</sub>/TiO<sub>2</sub> composite films coated on glass fibers. The films were also characterized for their morphology, anatase crystallinity, and band gap energy and considered fundamental explanatory characteristics affecting photocatalytic activity.

## 2. Experimental

### 2.1 Materials and methods

Three coating layers were deposited on glass fibers of type E-glass by the sol-gel process using the dip-coating method. The specific surface area of the starting glass fiber materials was 0.05 m<sup>2</sup>g<sup>-1</sup> and the diameter was about 20 μm. The coating sol for the first layer film was a SiO<sub>2</sub>/TiO<sub>2</sub>, prepared by dissolving 9 mL titanium tetra-isopropoxide (TTIP, 99.95%, Fluka Sigma-Aldrich) and 0.07 mL tetraethylorthosilicate (TEOS, 98%, Fluka Sigma-Aldrich) with 145 mL ethanol, stirring at room temperature at a speed of 800 rpm for 60 min to achieve the mole ratio of TTIP:C<sub>2</sub>H<sub>5</sub>OH = 1:82, then adding 2 M HCl into the sol to adjust pH to be about 3.5. The coating sol for the second and third layers were the N-doped SnO<sub>2</sub>/TiO<sub>2</sub> composite, prepared by dissolving certain amounts of TTIP, polyvinylpyrrolidone (PVP), and 0.315 g tin (IV) chloride pentahydrate (98%, Riedel DeHaën) with 145 mL ethanol, stirring at room temperature at a speed of 800 rpm for 60 min then adding 2 M HCl into the sol to adjust pH to be about 3.5. The concentration of SiO<sub>2</sub> in TiO<sub>2</sub> of the first layer was fixed at 5 mol%, while in the second and third layer 3 mol% SnO<sub>2</sub> was used [9]. From our previous study the nitrogen of 40 mol% was selected to dope into the SnO<sub>2</sub>/TiO<sub>2</sub> films since it exhibits the higher photoactivity compared to other concentrations [10].

Before coating, the glass fibers were heated at 500°C for 1 h in order to remove wax, it was then cleaned in an ultrasonic bath by using ethanol and dried at 105°C for 24 h. A dip-coating apparatus was used to coat the fibers. Firstly, SiO<sub>2</sub>/TiO<sub>2</sub> sol was coated on glass fibers as a compatibilizer layer and followed with N-doped SnO<sub>2</sub>/TiO<sub>2</sub> sol on top for another two layers. The

sol was homogenously coated on the substrate at the dipping speed of 1.0 mm/s. Secondly, gel films of TiO<sub>2</sub> composites were obtained by drying at 60°C for 30 min before calcination at 600°C for 2 h at a heating rate of 10°C/min. After that the TiO<sub>2</sub> composite films coated glass fibers were cleaned with distilled water in an ultrasonic bath for 15 min in order to remove the TiO<sub>2</sub> free particles, dried at 105°C for 24 h and kept in a desiccator until use in experiments [10].

## 2.2 Materials characterization

The surface morphology of the prepared films were characterized by scanning electron microscopy (SEM, Quanta, FEI ) and atomic force microscopy (AFM) Multi-Mode scanning probes Veeco NanoScope IV with a scan area of 2 μm × 2 μm. Crystallinity composition was characterized by using an X-ray diffractometer (XRD) (Phillips E'pert MPD, Cu-Kα). The crystallite size was determined from XRD peaks using the Scherer equation [11],

$$D=0.9\lambda/\beta\cos\theta_{\beta} \quad (1)$$

where D is crystallite size, λ is the wavelength of X-ray radiation (Cu-Kα = 0.15406 nm), θ is the Bragg's angle and β is the full width at half-maximum (FWHM). The band gap energies of TiO<sub>2</sub> and TiO<sub>2</sub> composites, in powder form, were measured by UV-Vis-NIR Spectrometer with an integrating sphere attachment (Shimadzu ISR-3100 spectrophotometer), by using BaSO<sub>4</sub> as reference.

## 2.3. Photocatalytic reactor

A schematic diagram of the photocatalytic reactor installation is shown in Fig. 1 (a and b). The main component of the installation was a photocatalytic reactor (Fig 1(c)).The water treatment reactor consisted of cylinder structure (1) that is made from acrylic. The photocatalytic reactor had the acrylic tubes in row (4 rows; 80 tubes) (3) and the outer part of the reactor had a black light lamp (5,7) that is source of UV light (10 watt; 20 tubes). The tube (3) has a capacity of at least 170 mL that is made from acrylic. The inside of the tube filled with 40N/SnO<sub>2</sub>/TiO<sub>2</sub> films immobilized on glass fibers calcined at 600°C (50 g) [10]. The photocatalytic reactor has structure that is made from acrylic (1). The inside of the reactor has the acrylic in row (3). The acrylic tube was closed with rubber stopper and serial connecting with rubber tube top (4) for continuous water flow through each tubes.

## 2.4 Photocatalytic experiments

Photocatalytic activity in motivate TiO<sub>2</sub> coated on glass fibers for water treatment. To examine the photocatalytic performance of the reactor, humic acid, fulvic acid, 2,4-dichlorophenol and glyphosate were used as model persistent organic compounds and the decomposition experiments of these compounds were carried out. All the solution was pumped into the reactor using a peristaltic pump with flow rate of 250–1,800 mL/min. The concentrations of humic acid, fulvic acid and 2,4-dichlorophenol used in this experiment was 10 mg/L for glyphosate used 1x10<sup>-4</sup> M. After that, when a solution concentration in the outlet was reached to an equilibrium concentration, photocatalytic degradation was initiated by starting the UV light irradiation (200 watt). The treated water was sampled periodically at the outlet, and the solution concentration changed as a function of time was determined by measuring with a UV-Vis spectrophotometer (UV-1700, Shimadzu, Japan). The photocatalytic activity of 5 samples was tested and an averaged value was taken for evaluation.

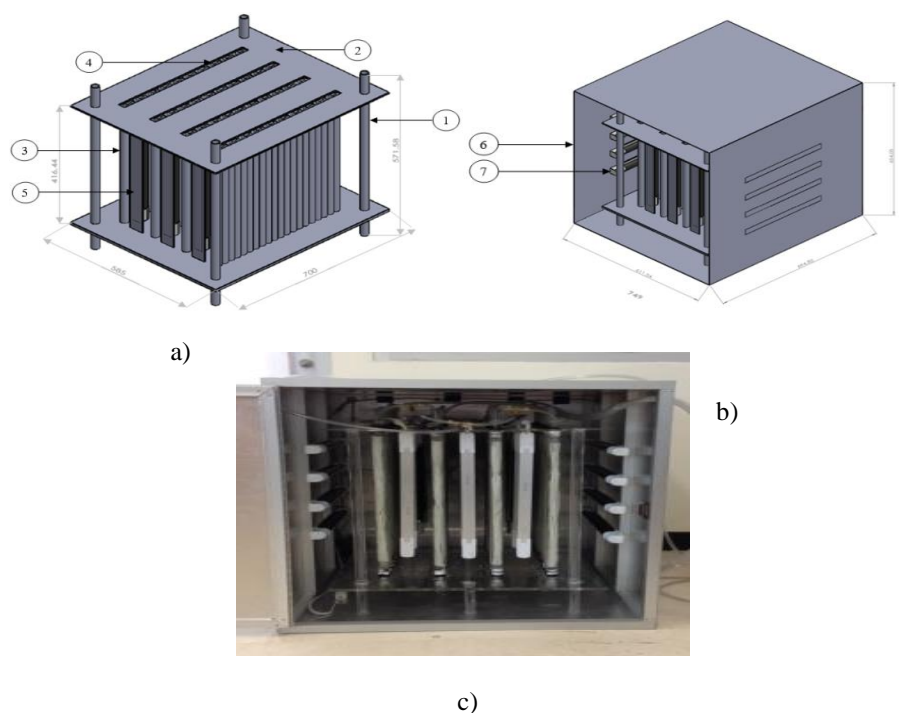


Fig. 1. (a,b) schematic diagram 1. cylinder structure, 2. acrylic plate, 3. acrylic tube, 4. rubber tube, 5,7. UV Light source, 6. aluminium wall and (c) photograph of photocatalytic reactor used in this study.

### 3. Results and discussion

#### 3.1 XRD Result of TiO<sub>2</sub> thin films

The XRD patterns of TiO<sub>2</sub>, along with undoped and N-doped SnO<sub>2</sub>/TiO<sub>2</sub> thin films, after calcination at 600°C for 2 h, are shown in Fig.2. Comparisons with the JCPDS 21-1272 anatase card of ASTM (American Society for Testing and Materials), and the JCPDS 21-1276 rutile ASTM card, suggest that all samples had anatase phase. The peaks correspond with different crystallographic planes against an almost flat base line suggest the formation of polycrystalline compounds [12]. The very broad diffraction peaks at (1 0 1) plane ( $2\theta = 25.3^\circ$ ) of N-doped SnO<sub>2</sub>/TiO<sub>2</sub> thin films were due to small crystallite size of TiO<sub>2</sub>. The crystallite sizes calculated from Scherrer's equation are shown in Table 1. It is well known that particle sizes play a vital role in photocatalytic activity since smaller crystals offer greater surface area to volume ratios and thus induce better surface absorbability of hydroxyl/water, which in-turn acts as an active oxidizer in the photocatalytic reaction [13] The relatively broad peaks of the XRD patterns imply the small crystallite size of anatase [14]. Nitrogen seems to hinder phase transformation from amorphous to anatase, as 40N/SnO<sub>2</sub>/TiO<sub>2</sub> film had the lowest degree of crystallinity. It can therefore be concluded that the level of nitrogen-doping has a significant effect on the crystallite size of TiO<sub>2</sub> grown during the doping process. It is known that both crystallite size and degree of crystallinity affect photocatalytic activity, so these physical characteristics corroborate the potential of N-doping for such effects.

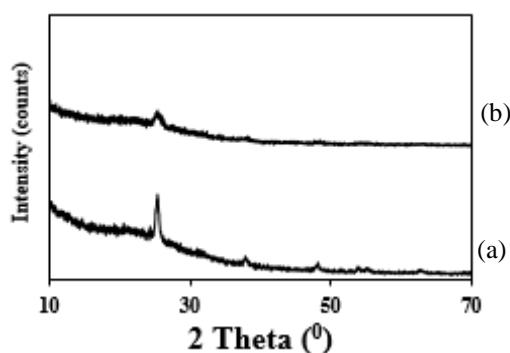


Fig. 2. XRD patterns of thin films: (a)  $\text{TiO}_2$  and (b) 40 mol%  $\text{N}/\text{SnO}_2/\text{TiO}_2$ .

Table 1. Crystallite sizes and energy band gaps of the calcined thin films synthesized.

Samples	Crystallite size (nm)	Energy band gap (eV)
$\text{TiO}_2$	17.2	3.20
40N/ $\text{SnO}_2/\text{TiO}_2$	8.6	2.94

### 3.2 Morphology of thin film surface

The morphology of  $\text{TiO}_2$  films coated on glass fibers were observed by SEM as illustrated in Fig. 3. It can be seen that the anatase crystallinity nucleated is homogeneous and has a smooth surface. However, excess  $\text{TiO}_2$  seems to be randomly deposited on glass fiber surfaces. Agglomeration of nanoparticles was clearly found for  $\text{TiO}_2$  film (Fig. 3 (b)). It can be seen that the anatase crystallinity nucleated is homogeneous and has a smooth surface (Fig. 3 (d)). PVP doping hindered the anatase crystal growth and reduced the crystallite size in agreement with the XRD results shown in Fig. 1.

The morphology of the composite  $\text{TiO}_2$  thin film coated surface observed by AFM is illustrated in Fig. 4. It can be seen that crystals of the anatase phase nucleated from the thin film are homogeneous. The average surface roughness of 40N/ $\text{SnO}_2/\text{TiO}_2$  thin film found from AFM images are about 2 nm. It was noted that the grain sizes of pure  $\text{TiO}_2$  and 40N/ $\text{SnO}_2/\text{TiO}_2$  films are estimated by AFM images about 40–50 and 20–30 nm, respectively. This smallest grain size affected by nitrogen-doping promoted the great photocatalytic activity of the 40N/ $\text{SnO}_2/\text{TiO}_2$  film.

### 3.4 Band gap energy determination

The UV–vis spectra of pure  $\text{TiO}_2$  and composite  $\text{TiO}_2$  are shown in Fig. 5. The absorption edge of the samples was determined by the following equation,

$$E_g = 1239.8/\lambda \quad (2)$$

where  $E_g$  is the band gap energy (eV) of the sample and  $\lambda$  (nm) is the wavelength of the onset of the spectrum. The undoped  $\text{TiO}_2$  catalyst exhibited absorption only in the UV region with the absorption edge around 400 nm. The band gap energies of the N-doped  $\text{SnO}_2/\text{TiO}_2$  catalysts listed in table 1 were slightly narrower than that of the undoped  $\text{TiO}_2$  (3.20 eV). Dopants affected the UV–vis spectra by inhibiting recombination of electron–hole pairs, here especially for the N-doped specimens. The band gap energy of N- $\text{SnO}_2/\text{TiO}_2$  was shifted by 0.14–0.26 eV relative to 3.20 eV for pure  $\text{TiO}_2$ . The band gap energy of 40N/ $\text{SnO}_2/\text{TiO}_2$  was 2.94 eV. The band gap energy of  $\text{TiO}_2$  tended to decrease with increasing N content. These shifts demonstrate how photocatalytic

activity may be modulated by atomic-level doping of a nano-catalyst. The absorption wavelength of the 40N/SnO<sub>2</sub>/TiO<sub>2</sub> photocatalyst is extended towards visible light ( $\lambda = 421.7$  nm), relative to the other samples [15], giving it the highest photocatalytic activity. The N-doping slightly decreased the band gap to 2.94 eV by the formation of localized N 2p states just above the valence band maximum of TiO<sub>2</sub>, due to substitutional N species [16]. When the amount of N-doping increased, the degree of crystallinity of anatase (TiO<sub>2</sub>) decreased, resulting in a reduction of crystallite size. In addition, the N interstitial atoms incorporated into the TiO<sub>2</sub> lattice had an effect on the light absorption edge shifting to longer wave length in visible region, leading to the reduction of band gap energy.

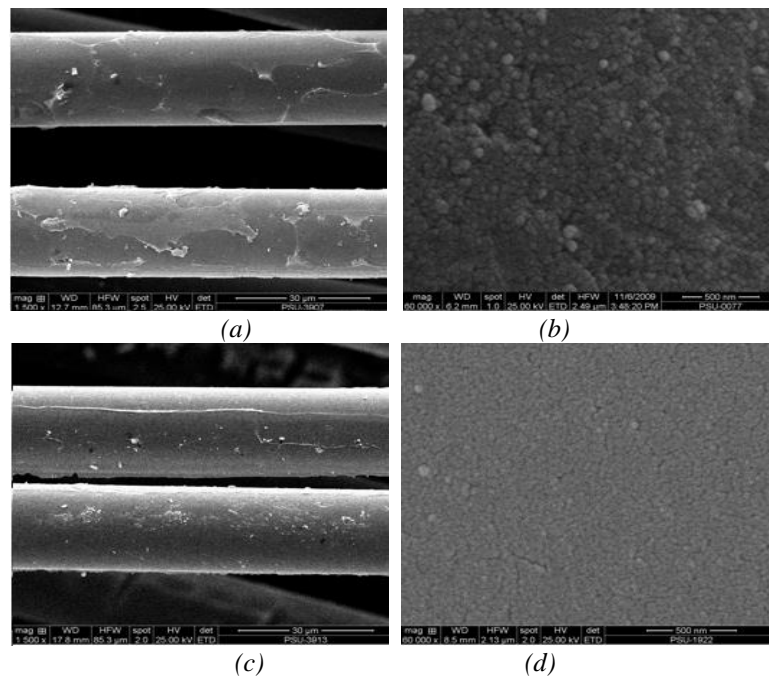


Fig. 3. SEM images of glass fibers, some coated (a) TiO<sub>2</sub> 1,500x, (b) TiO<sub>2</sub> 60,000x, (c) 40N/SnO<sub>2</sub>/TiO<sub>2</sub> 1,500x, and (d) 40N/SnO<sub>2</sub>/TiO<sub>2</sub> 60,000x.

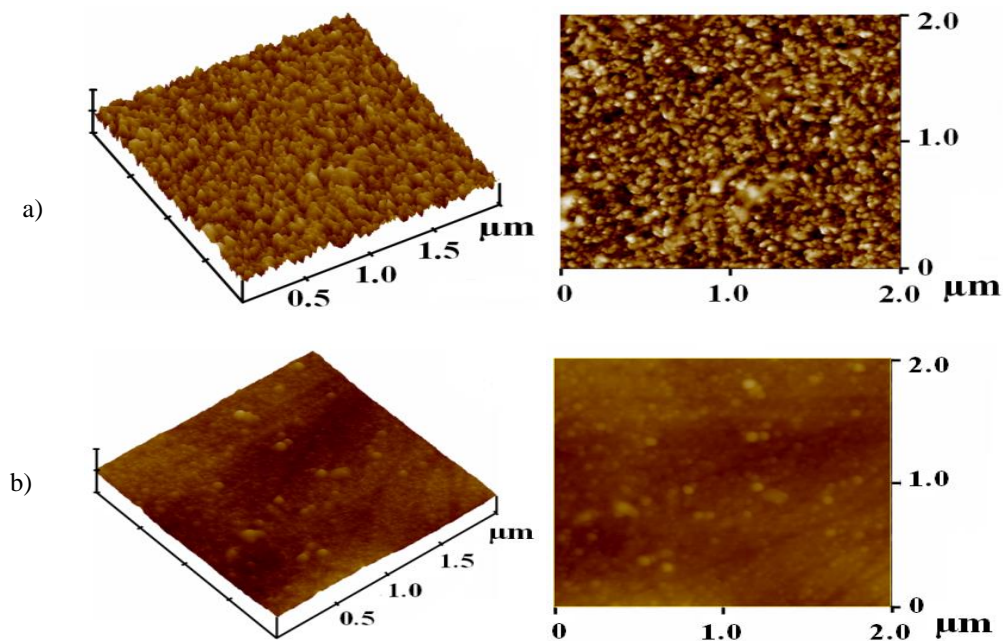


Fig. 4. AFM image with a scan area of  $2 \times 2$  μm of (a) pure TiO<sub>2</sub>, (b) 40N/SnO<sub>2</sub>/TiO<sub>2</sub> films coated on glass fibers.

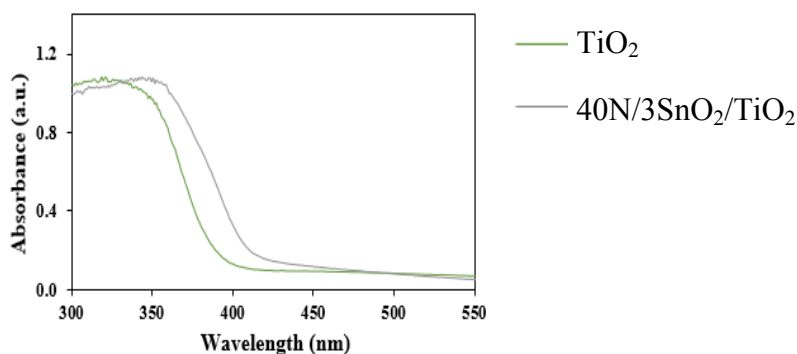


Fig. 5. UV-Vis diffuse reflectance spectra of pure  $\text{TiO}_2$  and  $40\text{N}/3\text{SnO}_2/\text{TiO}_2$  samples.

### 3.6 Photocatalytic activity test

The photocatalytic activities of the films on glass fibers were determined for degradation of humic acid, fulvic acid, 2,4-dichlorophenol and glyphosate under UV light for various flow rates (Fig. 6). The 250 mL/min flow rate had optimal photocatalytic activity across the range of flow rates tested. Doping  $\text{TiO}_2$  with a suitable amount of nitrogen (40 mol%) in  $\text{SnO}_2/\text{TiO}_2$  composite films shifted light absorption wavelength to the visible region, reduced crystallite size to be about 8.6 nm, and narrowed the energy band gap to 2.94 eV (Table 1) [17]. It was found that at the flow rate of 250 mL/min the photoreactor degradation of humic acid, fulvic acid, glyphosate and 2,4-dichlorophenol were 91.30, 95.50, 71.80 and 88.70 %, respectively. At the flow rate of 1,800 mL/min the photoreactor degradation of humic acid, fulvic acid, glyphosate and 2,4-dichlorophenol were 78.3, 67.5, 56.8 and 43.9, respectively. The degradation efficiency, was the highest at 95.50% for fulvic acid compared with other contamination on the complexity of the molecule. The texture characteristics show that glass fibers have high interaction and apparent surface area. It will normally produce a lower reaction when high water flow rate due to low surface contact between reactants.

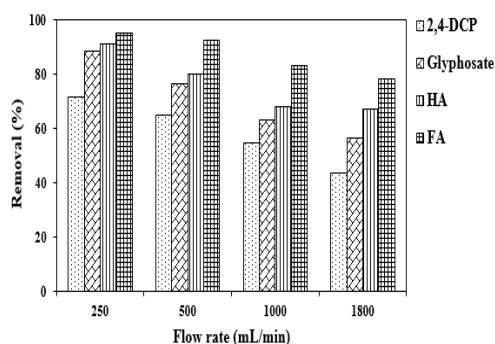


Fig. 6. Photocatalytic degradation of humic acid ( $C_0 = 10 \text{ mg/L}$ ), fulvic acid ( $C_0 = 10 \text{ mg/L}$ ), 2,4-dichlorophenol ( $C_0 = 10 \text{ mg/L}$ ), and glyphosate ( $C_0 = 1 \times 10^{-4} \text{ M}$ ), under UV light for various flow rates.

## 4. Conclusions

N-doped  $\text{SnO}_2/\text{TiO}_2$  composite films were successfully synthesized and deposited on glass fibers, via sol-gel and dip-coating methods. The coated fibers were calcined at  $600^\circ\text{C}$  for 2 h at a heating rate of  $10^\circ\text{C}/\text{min}$  in order to form crystalline anatase. N-doping of  $\text{SnO}_2/\text{TiO}_2$  composite films affected surface smoothness, crystallite size, and band gap energy of the films. The synergistic effects of N and  $\text{SnO}_2$  co-doping with a suitable amount are responsible for the high photo-activity due to their effect on smaller crystallite size and narrower band gap energy of these

TiO<sub>2</sub> composite films. It was found that at the flow rate of 250 mL/min the photo-reactor degradation rate of humic acid, fulvic acid, glyphosate and 2,4-dichlorophenol contamination in drinking water were 91.30, 95.50, 71.80 and 88.70 %, respectively. It is apparent that TiO<sub>2</sub> composite photocatalytic reactor shows advantages in degradation of some hazardous chemical compounds contaminated in water.

### Acknowledgments

The authors would like to thank the Department of Materials Engineering, Faculty of Engineering and Architecture, Rajamangala University of Technology Isan for supporting this work. Dr. Mcwinner Yawman is also acknowledged for his comments and suggestions, as he is the Research & Publication Expert and Trainer of the Institute of Research and Development Rajamangla University of Technology Isan.

### References

- [1] K. Lee, H. Ku, D. Pak, *Chemosphere* **149**, 114 (2016).
- [2] S. Mozia, P.B. Zek, P. JacekÓrski, B. Tryba, A.W. Morawski, *J. Nanomater.* **2012**, 1 (2012).
- [3] J. Ida, T. Watanabe, S. Watanabe, T. Matsuyama, H. Yamamoto, *Sep. Purif. Technol.* **134**, 66 (2014).
- [4] H. Tada, Y. Konishi, A. Kokubu, S. Ito. *Langmuir* **20**(9), 3816 (2004).
- [5] A. Kadam, R. Dhabbe, D.S. Shin, K. Garadkar, J. Park, *Ceram. Int.* **43**(6), 5164 (2017).
- [6] M. Zhou, J. Yu, S. Liu, P. Zhai, L. Jiang, *J. Hazard. Mater.* **154**(1–3), 1141 (2008).
- [7] C. D. Valentin, E. Finazzi, G. Pacchioni, A. Sellonib, S. Livraghi, M.C. Paganini, E. Giamello, *Chem. Phys.* **339**(1–3), 44 (2007).
- [8] J. Georgieva, E. Valova, S. Armyanov, D. Tatchev, S. Sotiropoulos, I. Avramova, N. Dimitrova, A. Hubin, O. Steenhaut, *Appl. Surf. Sci.* **413**(15), 284 (2017).
- [9] P. Kongsong, L. Sikong, S. Niyomwas, V. Rachpech, *Key Engineering Materials* **608**, 164 (2014).
- [10] P Kongsong, L. Sikong, M. Masae, *EnvironmentAsia* **10**(2), 126 (2017).
- [11] Z. Liuxue, L. Peng, S. Zhixing, *Mater. Chem. Phys.* **98**(1), 111 (2006)
- [12] M. Thomas, S. K. Ghosh, K.C. George, *Mater. Let.* **56**(4), 386 (2002).
- [13] G. Yang, Z. Jiang, H. Shi, T. Xiao, Z. Yan. *J. Mater. Chem.* **20**(25), 5301 (2010).
- [14] D. Wang, L. Xiao, Q. Lau, X. Li, J. An, Y. Duan, *J. Hazard. Mater.* **192**(1), 150 (2011).
- [15] L. Sikong, M. Masae, K. Kooptarnond, W. Taweepreda, F. Saito, *Appl. Surf. Sci.* **258**(10): 4436 (2012).
- [16] R. Jaiswal, N. Patel, D. C. Kothari, A. Miotello, *Appl. Catal. B* **126**, 47 (2012).
- [17] J. Ying, H. Bai, Q. Jiang, J. Lian, *Thin Solid Films* **516**(8), 1736 (2008).